Self-assembly of supramolecular nanostructures from phenylalanine derived bolaamphiphiles†

Monica Z. Menzenski and Ipsita A. Banerjee*

Received (in Durham, UK) 19th February 2007, Accepted 8th May 2007
First published as an Advance Article on the web 19th June 2007
DOI: 10.1039/b702586f

The growth and self-assembly of phenylalanine derived bolaamphiphiles was investigated. The self-assembly process was studied at hydrophobic–hydrophilic interfaces and under aqueous conditions at different pH. The formation of various structures in microscale and nanoscale was examined using atomic force microscopy, transmission electron microscopy, dynamic light scattering, ultraviolet-visible spectroscopy and infrared spectroscopy. It was observed that the types of structures formed were dependent on both the growth conditions and the chain lengths of the hydrocarbons linking the head groups. At lower pH, tubular formations were observed in high yield for all bolaamphiphiles synthesized compared to higher pH. As the size of the hydrophobic chain length connecting the amino acid head groups increased, the nanotubes were formed in higher yield and were observed to be more elongated and well-defined. In some cases, nanofibers, spheres and rod-like structures were also obtained at aqueous/organic interfaces and in different pH. The investigation of the self-assembly process of such peptide bolaamphiphiles can give further insight into the dynamics of formation of various supramolecular structures. The materials formed were found to be highly stable and can be potentially used as scaffolds for biomaterials and fabrication of nanodevices.

Introduction

Molecular self-assembly has been gaining much popularity for its use in the design and fabrication of various structures leading to the formation of novel nanomaterials. The self-assembly process plays a vital role in the discovery of new materials and scaffolds, with an extensive range of applications in nanotechnology and medical technologies such as regenerative medicine and drug delivery systems.[1] The formation of intricate multicomponent three-dimensional structures occurs from the natural association of molecules arbitrated through weak intermolecular forces, such as van der Waals forces, electrostatic interactions, hydrogen-bonding, various stacking interactions, and ultimately leads to integral and efficient supramolecular structures.[2]

Amphiphilic molecules consist of hydrophobic and hydrophilic moieties within the same molecule that can self-assemble into various morphologies, including micelles, rods, tubes and vesicular aggregates. Such molecules self-assemble into these distinct morphologies depending on initial conditions such as concentration, pH and temperature[3] and can function as templates for the nucleation, growth and deposition of inorganic substances allowing for mineralization with metals such as nickel, palladium, copper, alumina and silica.[4] A class of ionic self-complementary peptides that spontaneously self-assemble in the presence of monovalent cations to form interlaced nanofibers was recently discovered.[1] These structures formed a hydrogel composed of peptides with alternating hydrophobic and hydrophilic amino acids. The self-assembly of these peptides was driven by electrostatic and hydrophobic interactions. Such self-assembling peptide scaffolds have been utilized as novel biomaterials for tissue-cell attachment, extensive neurite outgrowth and construction of active nerve connections.[1] In some cases self-assembly of peptide hydrogels have also been induced photochemically or thermally.[5]

The importance of channels in sustaining biological systems and their potential benefits in nanotechnology and biomedicine has furthered the investigation of the structure-function relationship.[6] Cyclic peptides composed of alternating D- and L-amino acids self-assemble into nanotubular structures exhibiting potential applications for the formation of inorganic nanocluster composites, biologically relevant transmembrane channels and pore assemblies on solid surfaces generating ion sensor devices.[7] The assembly, orientation and structural characteristics of nanotubes composed of the cyclic peptides *cyclo*-[(L-Phe-D-*N*-MeAla-)$_4$], *cyclo*-[(L-Trp-D-Leu)$_3$-L-Ser-D-Leu] and *cyclo*-[(L-Trp-D-Leu)$_4$] formed at the air/water interface have been studied. For example, the peptide *cyclo*-[(L-Trp-D-Leu)$_3$-L-Ser-D-Leu] created mostly planar aggregates consisting of several tubes oriented with their long axes parallel to the air–water interface.[7] A synthetic channel system composed of a tubular collection of stacked cyclic peptides composed of *cyclo*-[(L-Trp-D-Leu)$_3$-L-Gln-D-Leu] was shown by vesicular arrays and single channel conductance

---

Fordham University, Department of Chemistry, Bronx, New York, USA. E-mail: banerjee@fordham.edu; Fax: 718-817-4432; Tel: 718-817-4445

† Electronic supplementary information (ESI) available: Kinetics of formation of self-assembled stuctures. Fig. S1: (a) Spherical structures formed after 2 days; (b) structures observed after 7 days in high pH using 1,3-bis(*N*-α-amido-Phe)propyl dicarboxylate at pH 9. Fig. S2: Formation of tubules observed after 5 days, using 1,7-bis(*N*-α-amido-Phe)heptyl dicarboxylate at pH 4. See DOI: 10.1039/b702586f

measurements to function as a transmembrane channel for ion and biomolecule transport. The design of this tubular structure was based on the claim that cyclic peptides of an even number of alternating D-and L-amino acids can assume a low-energy, flat-ring conformation in which the hydrogen-bonding backbone moieties are oriented perpendicular to the plane of the ring and the side chains are positioned radially away from the ring. Such a conformation enabled the cyclic peptide units to self-assemble into an antiparallel β-sheet-like cylindrical structure and to theoretically function as membrane-spanning channels.[6]

In general, organic tubular assemblies comprise a growing category of supramolecular structures with promising applications in chemical and biological settings. Among various approaches utilized for the development of organic nanotubes, the hydrogen-bonded self-assembly of macrocyclic ring formations has been demonstrated to be predominantly useful. Sequential condensation and deprotection of appropriately protected amino acids provide a simplistic path for synthesis of the assembling subunits. The number and sequence of amino acids used defines the diameter and surface properties of the tubular assembly.[8] It has been shown that the functional characteristics of such organic nanotubes depend on both their internal and external surfaces. The hydrophilic aspect of the peptide nanotube interior has been an essential feature in designing transmembrane ion channels and pores. Variation of the internal properties require peptide main-chain replacements with hydrophobic moieties that favourably affect the conformational circumstances of the subunit for self-assembly by means of intermolecular hydrogen-bonding.[8] Recently, peptide nanotubes were formed using the D-Phe-D-Phe dipeptide. This motif self-assembled into long and rigid structures with proteolytic liability.[2]

Nanostructures self-assembled from peptide bolaamphiphiles (amino acid head groups covalently bound *via* a hydrocarbon chain) exhibit several properties that make them a promising candidate including facile self-assembly and adaptability to functionalization and increased biocompatibility.[2,9–12] The peptide head groups can be readily modified in order to manipulate and potentially alter the properties of the self-assembled materials to be utilized for desired applications. Additionally, the length of the aliphatic chain intervening between the two peptide head groups of the bolaamphiphile may be tailored as well.[2,8,13,14] Recently, it has been shown that simple dipeptides such as D-Phe-D-Phe and L-Phe-L-Phe could be efficiently self-assembled into nanotubular structures.[2,15] However, the effect on the self-assembly process of phenylalanine derived bolaamphiphiles with varying chain lengths has not yet been investigated. Thus it would be interesting to study the consequence of varying the distance between the phenylalanine groups. Here we have synthesized a series of new peptide bolaamphiphiles containing a bis(*N*-α-amido-phenylalanine) dicarboxylate moiety. The hydrocarbon chain linking the phenylalanine amino acids was varied between three and ten carbons and the self-assembly of each of those materials was studied under varying conditions. The chemical structures of the bolaamphiphiles are shown in Fig. 1 and molecular models are shown in Fig. 2. Although phenylalanine itself is a relatively hydrophobic amino acid, the presence of the carboxylate groups provides the bolaamphiphiles with a polar constituent. The presence of the –CH_2 groups connecting the Phe–carboxylate head groups may further add to the hydrophobicity of the bolaamphiphiles. Since natural membrane proteins tend to assemble at hydrophobic–hydrophilic interfaces,[16,17] it would be beneficial to study the self-assembly of hydrophobic bolaamphiphiles such as those synthesized in this work under varying conditions. Thus, the self-assembly of the synthesized materials was investigated at aqueous/organic interfaces and in varying pH conditions. Our aim was to mimic the self-assembly of membrane proteins. Such self-assembled nanostructures can potentially be conjugated with appropriate materials and utilized for various applications such as in molecular electronics, drug delivery, and regenerative medicine.[15,18–22]

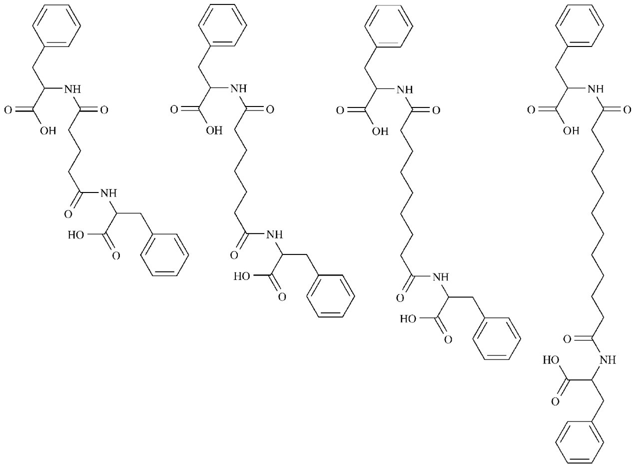

Fig. 1 The structures of the bolaamphiphiles synthesized: 1,*n*-bis-(*N*-α-amido-Phe) dicarboxylates (n = 3, 5, 7, 10).

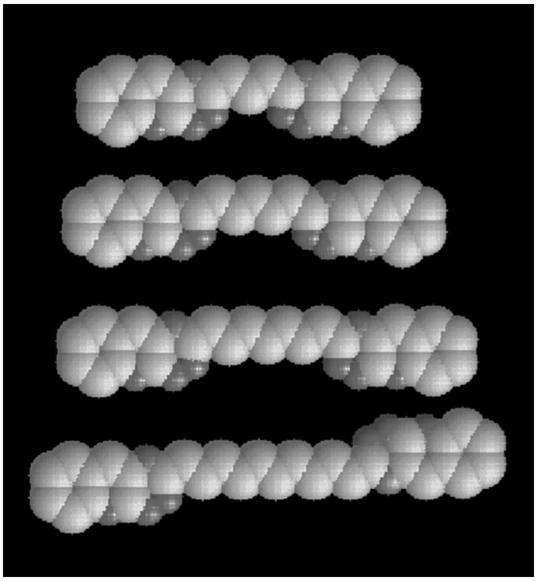

Fig. 2 Molecular models of the peptide bolaamphiphiles synthesized. From top to bottom the aliphatic –$(CH_2)_n$– groups connecting the phenylalanine amino acids, n = 3, 5, 7 and 10.

Results and discussion

To mimic natural biological systems, several peptide assemblies have been synthesized thus far.[1,2,23,24] It has been observed that in most cases, such assemblies are promoted by protonation and they are formed either instantaneously or over a period of time.[24] We have synthesized a series of new bolaamphiphiles, containing the HOOC–Phe–NH–CO–$(CH_2)_n$–CO–NH–Phe–COOH moiety. The bolaamphiphiles have two polar carboxylic acid groups attached to each of the phenylalanines and can be considered as the head groups. The alkyl spacer between the head groups was varied between three and ten methylene groups and can be considered as the tail groups. Thus, (n) was varied between three and ten carbons. The self-assembled structures are anticipated to be sensitive to pH due to the presence of the carboxyl groups. In addition, the presence of the Phe moiety would result in π–π stacking interactions. Following synthesis, the self-assembly process was studied under various conditions. The effects of structural variation of the monomers (different hydrophobic chain lengths) and the effects of external growth conditions (hydrophobic–hydrophilic interfaces and various pH) were systematically studied. In general, assemblies appeared within one-to-two weeks at room temperature. It was observed that the types of structures formed were dependent on both the growth conditions and the chain lengths of the hydrocarbons linking the head groups.

Effect of pH

For all bolaamphiphiles synthesized, it was observed that at lower pH (between 4 and 5), tubular and rod-like structures were observed after two weeks as shown in Fig. 3. Fig. 3(a) and (b) show the AFM and TEM images of the formed rod-like and tubular formations obtained from the self-assembly of the 1,5-bis(*N*-α-amido-Phe)pentyl dicarboxylate and 1,7-(*N*-α-amido-Phe)heptyl dicarboxylate moieties at pH 5, respectively. At higher pH, (greater than 7) more vesicle and donut-like structures were obtained as shown in Fig. 4. Fig. 4(a) and (b) show the AFM images of vesicles and donut-like nanostructures formed from the self-assembly of 1,5-(*N*-α-amido-Phe)-pentane dicarboxylate at pH 8 and 10, respectively. It should be noted that a similar trend was observed for the propyl and heptyl dicarboxylate moieties as well. These results suggest that pH of the growth solution plays a significant role in the self-assembly of the nanostructures. Such behaviour has also been observed for compounds such as benzoic diacid diamides which were found to form microspheres at pH 8 and tubular structures at pH 7.[25] In Fig. 4(b), some tubular aggregates appear to have self-assembled on the surface of the microspheres, producing a donut-like structure. At this point, the nucleation mechanism of these tubular structures on the surface of the donut like structures is unknown. Further structural studies of these materials would be necessary to probe the exact mechanism of formation. In this work, we have used infrared spectroscopy to elucidate the mechanism of formation of the various assemblies.

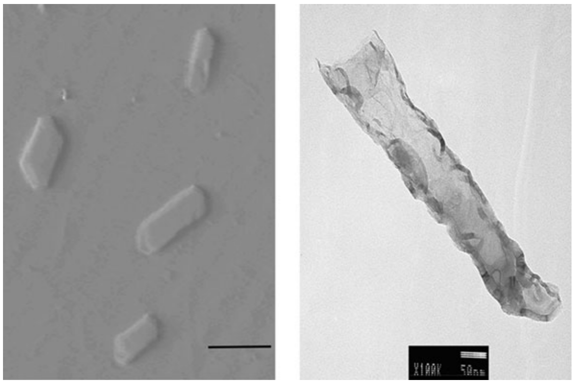

Fig. 3 (a) AFM image of rods formed using 1,5-bis(*N*-α-amido-Phe)pentyl dicarboxylate at pH 5 (scale bar = 2 μm). (b) TEM image of a tubule formed at pH 5 from 1,7-bis(*N*-α-amido-Phe)heptyl dicarboxylate.

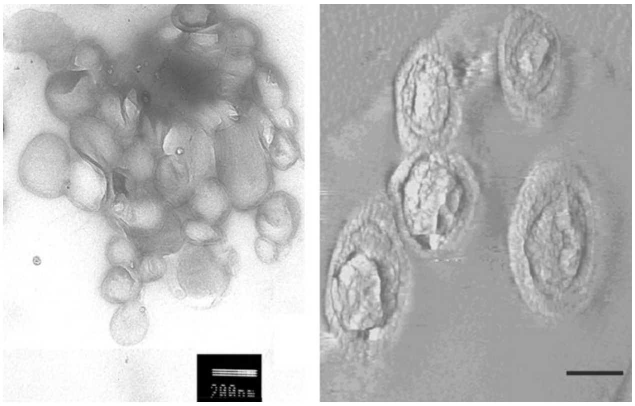

Fig. 4 (a) and (b) are TEM and AFM images of vesicles formed at pH 8 and donut-like structures formed at pH 10 (scale bar = 500 nm), respectively, from the 1,5-bis(*N*-α-amido-Phe)pentyl dicarboxylate.

Effect of aliphatic chain length

The length of the alkyl spacer most likely plays a key role in the hydrophobic interactions as well as the π–π stacking among the aromatic groups and consequently on the hydrogen-bonding pattern. The effect of the hydrocarbon spacer was studied by varying the sizes of the hydrocarbon spacer between three to ten carbons. In general, at low pH, as the size of the hydrophobic chain length connecting the amino acid head groups increased, the tubular structures were observed to be longer and more distinct in the order of micrometers (Fig. 5).

Sizes of nanostructures as obtained from DLS studies

In order to analyze the size range of the nanostructures formed under the various conditions, we performed DLS experiments. A size range of 20–40 nm (mean diameter = 23.5 nm) was observed for the bis(*N*-α-amido-Phe)propyl dicarboxylate moiety at pH 7 (Fig. 6(a)). In comparison, the size range of 50–90 nm (mean diameter = 61.3 nm) was observed for the bis(*N*-α-amido-Phe)pentyl dicarboxylate moiety at pH 7 (Fig. 6(b)). In both cases, the samples were found to be relatively polydisperse. This indicates that the diameters of the nanostructures formed are higher for the longer chain length compounds. It should also be noted that the DLS experiments were conducted after six months of growth, which

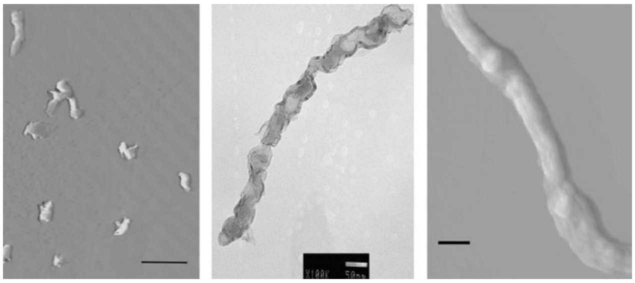

Fig. 5 (a) AFM image of tubular formations observed by self-assembly of 1,3-bis(*N*-α-amido-Phe)propyl dicarboxylate (scale bar = 4 μm); (b) TEM image of a nanotube obtained using 1,7-bis(*N*-α-amido-Phe)heptyl dicarboxylate (c) AFM image of a microtubule formed from 1,10-bis(*N*-α-amido-Phe)decyl dicarboxylate (scale bar = 2 μm).

would explain the polydispersity. This implies that the self-assembly and growth process are highly dynamic.

Growth under aqueous/organic conditions

The phenylalanine monomers were allowed to self-assemble in solutions containing a 1 : 1 ratio of hexane and deionized water. After two weeks, self-assembled structures were observed at the interfaces of the aqueous/organic solutions (Fig. 7). The 1,3-bis(*N*-α-amido-Phe)propyl dicarboxylate moiety resulted in the formation of short tubular structures as shown in Fig. 7(a), while the corresponding 1,5-bis(*N*-α-amido-Phe)pentyl dicarboxylate compounds resulted in the formation of long and stable fibers as illustrated in Fig. 7(b). The heptane and decane dicarboxylate moieties revealed aggregated fiber-like structures (data not shown).

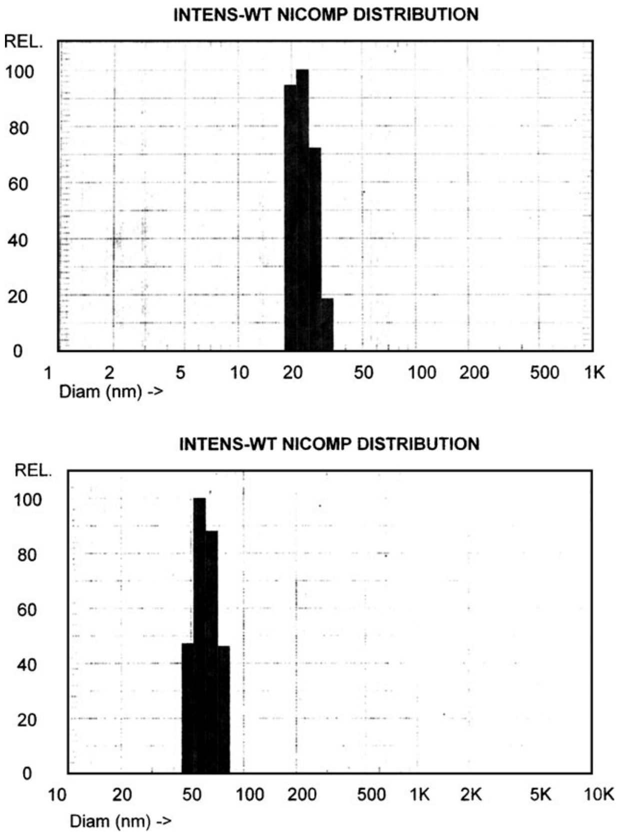

Fig. 6 (a) DLS studies of structures formed from 1,3-bis(*N*-α-amido-Phe)propyl dicarboxylate at pH 7 with a mean diameter of 23.5 nm. (b) DLS studies of structures formed from 1,5-bis(*N*-α-amido-Phe)pentyl dicarboxylate at pH 7 with a mean diameter of 61.3 nm.

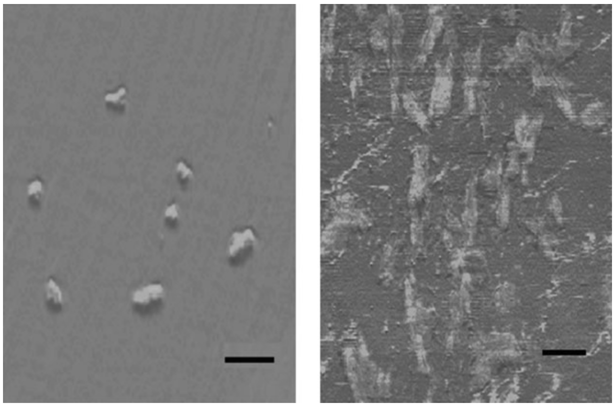

Fig. 7 (a) AFM image of short tubular formations formed from 1,3-bis(*N*-α-amido-Phe)propyl dicarboxylate at the aqueous/organic interface (scale bar = 1 μm). (b) AFM image of fibers formed using 1,5-bis(*N*-α-amido-Phe)pentyl dicarboxylate at the aqueous-organic interface (scale bar = 2 μm.

FT-IR spectroscopy

In order to probe the growth mechanism involved in the formation of the various assemblies and their hydrogen bonding patterns, FT-IR analyses of each of the structures grown under varying conditions were carried out. The spectra were compared with those of the synthesized monomers. The spectra obtained for the bolaamphiphiles with short aliphatic chain length ($n = 3$) are represented in Table 1, while those obtained for the longer aliphatic chain lengths, ($n = 10$) are represented in Table 2. The C=O stretch frequency shifts depend on the intermolecular hydrogen-bonding interactions between C=O and HN. From the results obtained, it appears that the IR spectra in the amide I and amide II regions are characteristic of significantly hydrogen-bonded, β-sheet-like networks as seen in the case of tubular structures observed at lower pH.[6,26] In addition, the N–H stretching frequencies occurring between 3172 and 3298 cm^{-1} also indicate strong intermolecular amide–amide bonds as indicated by the N–H (amide II) stretching mode tight hydrogen-bonding interactions. In all cases, the vibrations for the out of plane phenyl ring system were observed in the range of 680–698 cm^{-1}. The IR spectra indicate that the tubular assemblies formed from the shorter chain bolaamphiphiles have two C=O peaks at 1649 and 1667 cm^{-1} while those formed from the longer chain bolaamphiphiles show two C=O peaks at 1642 and 1661 cm^{-1}. The C=O stretch with the highest frequency is assigned as the free C=O of the amide group.[27] The lower C=O frequencies are red shifted compared to the free C=O stretch since those C=O groups are most likely bound to the amide NH group *via* intermolecular hydrogen-bonds. The non-tubular structures such as the donut-like structures and vesicles show a single peak for C=O stretch at 1652 and 1656 cm^{-1} for the short and the longer chain bolaamphiphiles, respectively.

Table 1 Vibrational frequencies (in cm^{-1}) and their peak assignments for 1,3-bis(*N*-α-amido-Phe)dicarboxylate monomer and self-assembled tubular and non-tubular structures

Peak assignment	Monomer of 1,3-bis(*N*-α-amido-Phe) dicarboxylate	Nanotubular structures at pH < 7	Nanostructures at pH > 7	Aqueous-organic interface
C=O (amide I) stretch	1643	1649 and 1667	1652	1653
N–H (amide II)	1585	1559	1587	1573
Alkyl C–H stretch	2851	2857	2853	2839
Carboxylic acid C=O stretch	1762	1733	1752	1759
Aromatic C–H bending	680	682	683	696
N–H stretch	3277	3277	3289	3298

Table 2 Vibrational frequencies (in cm^{-1}) and their peak assignments for 1,10-bis(*N*-α-amido-Phe) dicarboxylate monomer and self-assembled tubular and non-tubular structures

Peak assignment	Monomer of 1,10-bis(*N*-α-amido-Phe) dicarboxylate	Nanotubular structures at pH < 7	Nanostructures at pH > 7	Aqueous-organic interface
C=O (amide I) stretch	1646	1642 and 1661	1656	1643
N–H (amide II)	1545	1551	1572	1588
Alkyl C–H stretch	2814	2926	2938	2975
Carboxylic acid C=O stretch	1769	1740	1756	1760
Aromatic C–H bending	696	693	692	698
N–H stretch	3172	3246	3279	3290

These peaks suggest that the C=O group in the tubular nanostructures bind to the NH groups more strongly than to the C=O groups of the nanovesicles and spherical structures as there is a red-shift observed in the vibrational frequency. The carboxylic acid vibrational mode of the non-tubular structures are observed at 1752 cm^{-1} (n = 3) and 1756 cm^{-1} (n = 10), while the carboxylic acid in the tubular structures appears at 1733 cm^{-1} (n = 3) and 1740 cm^{-1} (n = 10). In the past, carboxylic acid vibrations in the acid–anion dimers have been observed around the 1740 cm^{-1} region in anionic lipids on membranes,[28] amphiphiles with glyconamide head-groups,[29] and many other bolaamphiphile assemblies.[24] The red shifted carboxylic acid frequency at 1730 and 1740 cm^{-1} in the tubular structures suggests that stronger acid–acid hydrogen-bonds (COOH–HOOC) may support the formation of tubular structures. The blue shifted carboxylic acid frequency in the case of vesicles indicates that the bolaamphiphiles most likely assemble due to the formation of anion–acid hydrogen-bonds at higher pH. Hydrophobic and electrostatic interactions due to the presence of the phenyl ring system as well as the alkyl chains may also contribute to the formation of the various nanostructures.

Absorbance spectroscopy

In order to further elucidate the driving forces and mechanisms for the formation of the various assemblies, absorbance spectroscopy measurements were conducted. The phenylalanine moieties induce rigidity to the structures and π–π stacking interactions are also involved.[30–34] The aliphatic chain length linking the head groups may possibly play an important role in altering the stacking interactions by varying the distance between the amino acid head groups. In general, π-conjugated materials have been applied as building blocks for developing organic-based devices[35] and their applications in electron-conducting polymers and light-emitting diodes usually involve assemblies from subunits by π–π stacking of two neighboring aromatic rings connected by linear flexible chains.[36–40]

To study the π–π stacking interactions, absorbance spectra of the monomer and the self-assembled structures were compared as shown in Fig. 8. In the case of the 1,7-bis(*N*-α-amido-Phe)heptyl dicarboxylate monomer, peaks were observed at 270 and at 225 nm. However, the peaks observed for those of the self-assembled structures were broader and significantly red-shifted. This indicates strong π–π stacking interactions both at organic-aqueous interfaces as well in aqueous conditions. In the case of the 1,3-bis(*N*-α-amido-Phe)propyl dicarboxylate monomer (Fig. 8(b)), in addition to a peak at 265 nm, a peak at 318 nm is also observed. This indicates that due to the proximity of the aromatic phenylalanine groups (because they are separated only by three methylene groups), there are intramolecular interactions involved within the molecule itself. However, upon self-assembly, broad red shifted peaks are observed which indicate intermolecular π–π interactions as well.

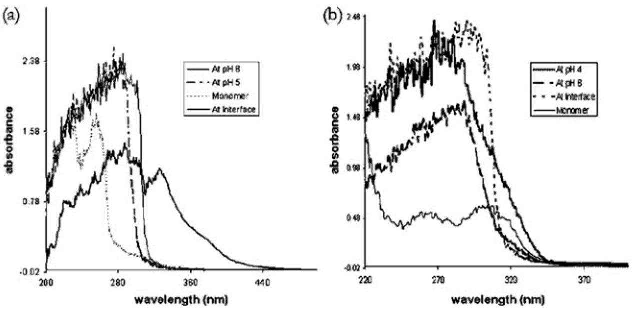

Fig. 8 (a) UV-Vis spectra obtained for 1,5-bis(*N*-α-amido-Phe)pentyl dicarboxylate and self-assembled structures. (b) UV-Vis spectra obtained for 1,3-bis(*N*-α-amido-Phe)propyl dicarboxylate and self-assembled structures.

Conclusions

Natural proteins utilize hydrogen bonding, electrostatic, van der Waals and hydrophobic interactions in directing three-dimensional folding arrangements. In the current work, we synthesized a series of bolaamphiphiles, containing the HOOC–Phe–NH–CO–$(CH_2)_n$–CO–NH–Phe–COOH moiety and evaluated the effectiveness of self-assembly into various nanostructures and microstructures by varying the connecting alkyl chain involved. The types of assemblies formed were dependent on both the growth conditions and the chain lengths of the hydrocarbons linking the amino acid head groups. As the size of the hydrophobic chain length connecting the amino acid head groups increased, tubular formations were formed in higher yield and were observed to be longer and more distinct in comparison to the shorter chain length compounds. In some cases, nanofibers and tubular structures were obtained at aqueous-organic interfaces as well. Thus, fine-tuning the structure of the precursor and the growth conditions can result in the formation nanostructures of pre-defined properties. Such materials can serve as very stable supramolecular scaffolds for fabrication of various nanoparticles and functional biomaterials.

Experimental

Materials

L-Phenylalanine benzyl ester hydrochloride, 1-hydroxybenzotriazole hydrate (HoBt), *N*-(3-dimethylaminopropyl)-*N*′-ethylcarbodiimide hydrochloride (EDAC), glutaric acid, pimelic acid, azelaic acid, dodecanedioic acid, solvents such as dimethylformamide, methanol, triethylamine, buffers and all other reagents were purchased from Sigma-Aldrich.

Synthesis of the bolaamphiphiles

The bolaamphiphiles were prepared according to previously established methods.[24] Briefly, the bolaamphiphile was synthesized by the coupling of the benzyl ester of the amino acid (1.2 g) with the appropriate dicarboxylic acid (0.65 g) (glutaric, pimelic, azelaic or dodecanedioic acid) at 0 °C in dimethylformamide (DMF). EDAC and 1-hydroxybenzotriazole were used as coupling agents and as additives, in that order. After 24 h, the DMF was rotoevaporated to give the intermediate, which was filtered and washed with citric acid (0.1 M) and sodium bicarbonate solutions (0.1 M). The intermediate was recrystallized from DMF in some cases. Finally, the ester groups were deprotected by catalytic hydrogenation or by base hydrolysis with NaOH at 92 °C. The products obtained ranged from pale yellow to white in color after washing with a 50 : 50 mixture of ice-cold water and acetone. ^1H NMR spectra were recorded with a Bruker 300 MHz NMR spectrometer for each sample.

Bis(*N*-α-amido-Phe)propyl dicarboxylate: ^1H NMR (DMSO-d_6): δ 1.7 (m, 2H), 2.8 (t, 4H), 5.1 (d, 4H), 7.5 (s, 10H) and δ 8.2 (d, 2H). Elemental analysis (%): C 64.18; H 6.1 N 6.4; O 22.3.

Bis(*N*-α-amido-Phe)pentyl dicarboxylate: ^1H NMR (DMSO-d_6): δ 1.4 (m, 2H), 1.7 (m, 4H), 2.5 (t, 4H), 8.1 (d, 2H), 7.3 (s, 10H), 5.2 (d, 4H). Elemental analysis (%): C 65.02; H 6.02; N 6.4; O 21.68.

Bis(*N*-α-amido-Phe)heptyl dicarboxylate: ^1H NMR (DMSO-d_6): δ 1.4 (m, 6H), 1.7 (m, 4H), 2.5 (t, 4H), 7.9 (d, 2H), 7.5 (s, 10H), 5.1 (d, 4H). Elemental analysis (%): C 65.6; H 6.92; N 6.2; O 20.98.

Bis(*N*-α-amido-Phe)decyl dicarboxylate: ^1H NMR (DMSO-d_6): δ 1.3 (m, 12H), 1.6 (m, 4H), 2.3 (t, 4H), 7.4 (s, 10H), 8.1 (d, 2H), 5.3 (d, 4H). Elemental analysis (%): C 68.5; H 7.7; N 5.2; O 18.2.

Self-assembly process

For the self-assembly process in aqueous solutions, individual stock solutions were prepared by adding 25.3 mg of the bis-(*N*-α-amido-Phe) dicarboxylate monomers to 5 mL buffer solutions ranging between pH 4 and 10. After 14 days of growth in different pH media, the peptide bolaamphiphiles self-assembled into various assemblies. The assemblies were sonicated (30 min) to dissociate any aggregates, washed with distilled water and centrifuged twice before being examined by TEM, optical microscopy and AFM.

For the self-assembly process in an aqueous/organic system, a stock solution of each of the monomers was prepared by adding 20 mg of the monomer to a 1 : 1 mixture of H_2O and hexane. The samples were vortexed for 20 min and then allowed to sit undisturbed for one-to-two weeks. The assemblies were sonicated (30 min) and examined by AFM. For examination, the samples were taken from the interface between the two liquids, pipetted out and dried.

Characterization

The particle sizes and morphologies of the samples were analyzed by atomic force microscopy (Quesant Q-scope), transmission electron microscopy and dynamic light scattering. The samples were washed twice with distilled water and air-dried on to carbon-coated copper grids for characterization by transmission electron microscopy (JEOL 120 EX) operated at 100 kV. Atomic force microscopy was carried out using a Quesant Universal SPM instrument in the tapping mode. The particle size ranges of the samples were analyzed by dynamic light scattering (NICOMP 380 ZLS).

Infrared spectroscopy

The nanostructures of the synthesized and self-assembled bis(*N*-α-amido-Phe) dicarboxylate bolaamphiphile monomers were analyzed by infrared spectroscopy. Fourier transform IR (FT-IR) spectra were recorded using Mattson Infinity FTIR infrared spectrophotometer in the range of 400–4000 cm^{-1}.

Absorption spectroscopy

The ultraviolet-visible absorption spectra were recorded using a Perkin-Elmer Model Lambda spectrophotometer in the range of 190–500 nm.

Acknowledgements

The authors thank Dr Areti Tsiola at the Queens College, CUNY Core facilities for Biomolecular Imaging for the use of the transmission electron microscope. I. B. thanks the

Fordham University Faculty Research Grant for financial support of this work.

References

1 (*a*) S. Vauthey, S. Santoso, H. Gong, N. Watson and S. Zhang, *Proc. Natl. Acad. Sci. U. S. A.*, 2002, **99**, 5355; (*b*) S. Zhang, T. Holmes, C. Lockshin and R. Rich, *Proc. Natl. Acad. Sci. U. S. A.*, 1993, **90**, 3334; (*c*) S. Zhang, *Nat. Biotechnol.*, 2003, **21**, 1171.
2 (*a*) M. Reches and E. Gazit, *Curr. Nanosci.*, 2006, **2**, 105; (*b*) G. M. Whitesides and B. Grzybowski, *Science*, 2002, **295**, 2418; (*c*) B. Hamelin, L. Jullien, C. Derouet, C. Hervé du Penhoat and P. Berthault, *J. Am. Chem. Soc.*, 1998, **120**(33), 8438; (*d*) M. Reches and E. Gazit, *Science*, 2003, **300**, 625; (*e*) C. H. Görbitz, *Chem. Commun.*, 2006, 2332.
3 T. Shimizu, M. Masuda and H. Minamikawa, *Chem. Rev.*, 2005, **105**, 1401.
4 (*a*) H. K. Baca, C. Ashley, E. Carnes, D. Lopez, J. Flemming, D. Dunphy, S. Singh, Z. Chen, N. Liu, H. Fan, G. P. López, S. M. Brozik, M. Werner-Washburne and C. J. Brinker, *Science*, 2006, **313**, 337; (*b*) F. Yu-Bin, Z. Li-De, Z. Ji-Yong and F. Shan-Gang, *Chin. J. Chem.*, 2004, **22**, 1142; (*c*) S. A. Davis, E. Dujardin and S. Mann, *Curr. Opin. Solid State Mater. Sci.*, 2003, **7**, 273; (*d*) A. M. Seddon, H. M. Patel, S. M. Burkett and S. Mann, *Angew. Chem., Int. Ed.*, 2002, **41**, 2988; (*e*) H. H. Paradies, M. Thies and U. Hinze, *Rigaku J.*, 2000, **17**, 9.
5 J. H. Collier, B.-H. Hu, J. W. Ruberti, J. Zhang, P. Shum, D. H. Thompson and P. B. Messersmith, *J. Am. Chem. Soc.*, 2001, **123**, 9463.
6 H. S. Kim, J. D. Hartgerink and M. R. Ghadiri, *J. Am. Chem. Soc.*, 1998, **120**, 4417–4421.
7 H. Rappoport, H. S. Kim, K. Kjaer, P. B. Howes, S. Cohen, J. Als-Nielsen, M. R. Ghadiri, L. Leiserowitz and M. Lahav, *J. Am. Chem. Soc.*, 1999, **121**, 1186.
8 W. S. Horne, C. D. Stout and M. R. Ghadiri, *J. Am. Chem. Soc.*, 2003, **125**, 9372.
9 R. Fairman and K. S. Akerfeldt, *Curr. Opin. Struct. Biol.*, 2005, **15**, 453.
10 H. Matsui, in *Encyclopedia of Nanoscience and Nanotechnolgy*, ed. H. S. Nalwa, American Scientific Publishers, Stevenson Ranch, CA, 2004, vol. 8, p. 445.
11 R. C. Claussen, B. M. Rabatic and S. I. Stupp, *J. Am. Chem. Soc.*, 2003, **125**, 12680.
12 T. Shimizu, *Macromol. Rapid Commun.*, 2002, **23**, 311.
13 J. H. Fuhrhop and T. Wang, *Chem. Rev.*, 2004, **104**, 2901.
14 M. R. Ghadiri, J. R. Granja, R. A. Milligan, D. E. Mcree and N. Khazanovich, *Nature*, 1993, **366**, 324.
15 (*a*) E. Gazit, *FEBS J.*, 2007, **274**, 317; (*b*) E. Gazit, *FASEB J.*, 2002, **16**, 77; (*c*) M. Reches and E. Gazit, *Nano Lett.*, 2004, **4**, 581.
16 M. G. Noro, M. A. Bates, A. Brisson and D. Frenkel, *Langmuir*, 2002, **18**, 2988.
17 G. V. Heijne, *Q. Rev. Biophys.*, 1999, **32**, 285.
18 N. Morino, K. Kitagawa, T. Morita and S. Kimura, *Thin Solid Films*, 2005, **479**, 261.
19 K. Goede, P. Busch and M. Grundmann, *Nano Lett.*, 2004, **4**, 2115.
20 N. C. Seeman and A. M. Belcher, *Proc. Natl. Acad. Sci. U. S. A.*, 2002, **99**, 6451.
21 I. A. Banerjee, L. Yu and H. Matsui, *Proc. Natl. Acad. Sci. U. S. A.*, 2003, **100**, 14678.
22 E. D. Sone and S. I. Stupp, *J. Am. Chem. Soc.*, 2004, **126**, 12756.
23 J. D. Hartgerink, T. D. Clark and R. M. Ghadiri, *Chem.–Eur. J.*, 1998, **4**, 1367.
24 M. Kogiso, S. Ohnishi, K. Yase, M. Masuda and T. Shimizu, *Langmuir*, 1998, **14**, 4978–4986.
25 H. Matsui and C. Holtman, *Nano Lett.*, 2002, **2**, 887.
26 (*a*) J. D. Hartgerink, J. R. Granja, R. A. Milligan and M. R. Ghadiri, *J. Am. Chem. Soc.*, 1996, **118**, 43–49; (*b*) A. Dong, J. Matsuura, M. C. Manning and J. F. Carpenter, *Arch. Biochem. Biophys.*, 1998, **355**, 275; (*c*) A. Dong, H. Huang and W. S. Caughey, *Biochemistry*, 1990, **29**, 3303.
27 H. Matsui and B. Gologan, *J. Phys. Chem. B*, 2000, **104**, 3383.
28 T. H. Haines, *Proc. Natl. Acad. Sci. U. S. A.*, 1983, **80**, 160.
29 J. H. Furlop, C. Demoulin, J. Rosenberg and C. Boettcher, *J. Am. Chem. Soc.*, 1990, **112**, 2827.
30 A. P. H. J. Schenning, P. Jonkheijm, E. Peeters and E. W. Meijer, *J. Am. Chem. Soc.*, 2001, **123**, 409.
31 C. A. Hunter and J. K. M. Sanders, *J. Am. Chem. Soc.*, 1990, **112**, 5525.
32 H. H. Perkampus, in *UV-Vis Spectroscopy and Its Applications*, Springer-Verlag, Berlin, 1992, ch. 7.
33 W. L. Jorgensen and D. L. Severance, *J. Am. Chem. Soc.*, 1990, **112**, 4768.
34 J. V. Herrikhuyzen, P. Jonkheijm, A. P. H. J. Schenning and E. W. Meijer, *Org. Biomol. Chem.*, 2006, **4**, 1539.
35 A. H. Tullo, *Chem. Eng. News*, 2000, **78**, 20.
36 J. D. Hartgerink, E. R. Subarev and S. I. Stupp, *Curr. Opin. Solid State Mater. Sci.*, 2001, **4**, 355.
37 L. M. Tumir, I. Piantanida, P. Novak and M. Zinic, *J. Phys. Org. Chem.*, 2002, **15**, 599.
38 T. Koizumi, K. Tsutsui and K. Tanaka, *Eur. J. Org. Chem.*, 2003, 4528.
39 S.-L. Deng, S. Y. Xie, X. Lu, Y.-B. Jiang, X.-L. Fang, R.-B. Huang and L. S. Zheng, *J. Mol. Struct.*, 2007, **829**, 51.
40 K. Avasthi, D. S. Rawat, P. R. Maulik, S. Sarkhel, C. K. Border and J. A. K. Howard, *Tetrahedron Lett.*, 2001, **42**, 7115.